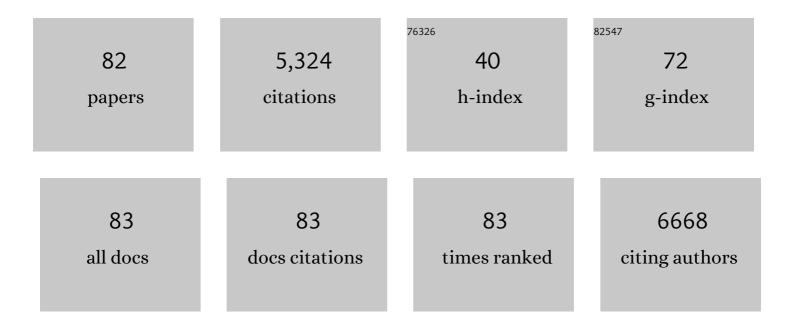
## Lisa M Miller

List of Publications by Year in descending order

Source: https://exaly.com/author-pdf/3790340/publications.pdf Version: 2024-02-01



#	Article	IF	CITATIONS
1	Synchrotron-based infrared and X-ray imaging shows focalized accumulation of Cu and Zn co-localized with β-amyloid deposits in Alzheimer's disease. Journal of Structural Biology, 2006, 155, 30-37.	2.8	521
2	Chemical imaging of biological tissue with synchrotron infrared light. Biochimica Et Biophysica Acta - Biomembranes, 2006, 1758, 846-857.	2.6	324
3	FTIR spectroscopic imaging of protein aggregation in living cells. Biochimica Et Biophysica Acta - Biomembranes, 2013, 1828, 2339-2346.	2.6	241
4	Low-level mechanical vibrations can influence bone resorption and bone formation in the growing skeleton. Bone, 2006, 39, 1059-1066.	2.9	218
5	The use of synchrotron infrared microspectroscopy in biological and biomedical investigations. Vibrational Spectroscopy, 2003, 32, 3-21.	2.2	204
6	In situ analysis of mineral content and crystallinity in bone using infrared micro-spectroscopy of the ν4 PO43â^ vibration. Biochimica Et Biophysica Acta - General Subjects, 2001, 1527, 11-19.	2.4	201
7	Beta-amyloid deposition and Alzheimer's type changes induced by Borrelia spirochetes. Neurobiology of Aging, 2006, 27, 228-236.	3.1	172
8	Accretion of Bone Quantity and Quality in the Developing Mouse Skeleton. Journal of Bone and Mineral Research, 2007, 22, 1037-1045.	2.8	138
9	Acetylesterase-Mediated Deacetylation of Pectin Impairs Cell Elongation, Pollen Germination, and Plant Reproduction Â. Plant Cell, 2012, 24, 50-65.	6.6	132
10	Increased brain iron coincides with early plaque formation in a mouse model of Alzheimer's disease. Neurolmage, 2011, 55, 32-38.	4.2	123
11	From structure to cellular mechanism with infrared microspectroscopy. Current Opinion in Structural Biology, 2010, 20, 649-656.	5.7	118
12	Amyloid plaques in PSAPP mice bind less metal than plaques in human Alzheimer's disease. NeuroImage, 2009, 47, 1215-1220.	4.2	117
13	Copper and Zinc Metallation Status of Copper-Zinc Superoxide Dismutase from Amyotrophic Lateral Sclerosis Transgenic Mice. Journal of Biological Chemistry, 2011, 286, 2795-2806.	3.4	112
14	Metal imaging in neurodegenerative diseases. Metallomics, 2012, 4, 721.	2.4	109
15	Chemical heterogeneity in cell death: Combined synchrotron IR and fluorescence microscopy studies of single apoptotic and necrotic cells. Biopolymers, 2003, 72, 366-373.	2.4	107
16	Identification of Conformational Substates Involved in Nitric Oxide Binding to Ferric and Ferrous Myoglobin through Difference Fourier Transform Infrared Spectroscopy (FTIR)â€. Biochemistry, 1997, 36, 12199-12207.	2.5	104
17	Amifostine, a radioprotectant agent, protects rat brain tissue lipids against ionizing radiation induced damage: An FTIR microspectroscopic imaging study. Archives of Biochemistry and Biophysics, 2012, 520, 67-73.	3.0	101
18	Synchrotrons versus globars, point-detectors versus focal plane arrays: Selecting the best source and detector for specific infrared microspectroscopy and imaging applications. Vibrational Spectroscopy, 2005, 38, 237-240.	2.2	97

#	Article	IF	CITATIONS
19	Tissue mineralization is increased following 1-year treatment with high doses of bisphosphonates in dogs. Bone, 2003, 33, 960-969.	2.9	93
20	FTIR-microspectroscopy of prion-infected nervous tissue. Biochimica Et Biophysica Acta - Biomembranes, 2006, 1758, 948-959.	2.6	77
21	In situ examination of the time-course for secondary mineralization of Haversian bone using synchrotron Fourier transform infrared microspectroscopy. Matrix Biology, 2008, 27, 34-41.	3.6	77
22	Combining high-resolution micro-computed tomography with material composition to define the quality of bone tissue. Current Osteoporosis Reports, 2003, 1, 11-19.	3.6	76
23	Rapid alignment of nanotomography data using joint iterative reconstruction and reprojection. Scientific Reports, 2017, 7, 11818.	3.3	75
24	In situ identification of protein structural changes in prion-infected tissue. Biochimica Et Biophysica Acta - Molecular Basis of Disease, 2003, 1639, 152-158.	3.8	72
25	In situ chemistry of osteoporosis revealed by synchrotron infrared microspectroscopy. Bone, 2003, 33, 514-521.	2.9	72
26	Determination of the oxidation states of manganese in brain, liver, and heart mitochondria. Journal of Neurochemistry, 2004, 88, 266-280.	3.9	71
27	Strontium ranelate does not stimulate bone formation in ovariectomized rats. Osteoporosis International, 2008, 19, 1331-1341.	3.1	69
28	Fourier Transform Infrared Imaging Showing Reduced Unsaturated Lipid Content in the Hippocampus of a Mouse Model of Alzheimer's Disease. Analytical Chemistry, 2010, 82, 2711-2716.	6.5	68
29	Comparison of Fourier transform infrared (FTIR) spectra of individual cells acquired using synchrotron and conventional sources. Infrared Physics and Technology, 2004, 45, 331-338.	2.9	64
30	Changes in intracortical microporosities induced by pharmaceutical treatment of osteoporosis as detected by high resolution micro-CT. Bone, 2012, 50, 596-604.	2.9	63
31	Enhancing digestibility and ethanol yield of Populus wood via expression of an engineered monolignol 4-O-methyltransferase. Nature Communications, 2016, 7, 11989.	12.8	61
32	Deletion of Cx43 from Osteocytes Results in Defective Bone Material Properties but Does Not Decrease Extrinsic Strength in Cortical Bone. Calcified Tissue International, 2012, 91, 215-224.	3.1	57
33	Chemical makeup of microdamaged bone differs from undamaged bone. Bone, 2006, 39, 318-324.	2.9	55
34	Metal-deficient aggregates and diminished copper found in cells expressing SOD1 mutations that cause ALS. Frontiers in Aging Neuroscience, 2014, 6, 110.	3.4	52
35	Elevated copper in the amyloid plaques and iron in the cortex are observed in mouse models of Alzheimer's disease that exhibit neurodegeneration. Biomedical Spectroscopy and Imaging, 2013, 2, 129-139.	1.2	50
36	In vitro efficiency and mechanistic role of indocyanine green as photodynamic therapy agent for human melanoma. Photodiagnosis and Photodynamic Therapy, 2009, 6, 105-116.	2.6	49

#	Article	IF	CITATIONS
37	Compositional characterization and imaging of "wall-bound―acylesters of Populus trichocarpa reveal differential accumulation of acyl molecules in normal and reactive woods. Planta, 2008, 229, 15-24.	3.2	45
38	Alterations in mineral composition observed in osteoarthritic joints of cynomolgus monkeys. Bone, 2004, 35, 498-506.	2.9	44
39	Imaging the Material Properties of Bone Specimens Using Reflection-Based Infrared Microspectroscopy. Analytical Chemistry, 2012, 84, 3607-3613.	6.5	43
40	Combining IR spectroscopy with fluorescence imaging in a single microscope: Biomedical applications using a synchrotron infrared source (invited). Review of Scientific Instruments, 2002, 73, 1357-1360.	1.3	42
41	Infrared imaging of compositional changes in inflammatory cardiomyopathy. Vibrational Spectroscopy, 2005, 38, 217-222.	2.2	42
42	Bisphosphonates do not alter the rate of secondary mineralization. Bone, 2011, 49, 701-705.	2.9	42
43	In situ characterization of prion protein structure and metal accumulation in scrapie-infected cells by synchrotron infrared and X-ray imaging. Vibrational Spectroscopy, 2005, 38, 61-69.	2.2	41
44	Low frequency vibrations of amino acid homopolymers observed by synchrotron far-ir absorption spectroscopy: Excited state effects dominate the temperature dependence of the spectra. Biopolymers, 1999, 49, 591-603.	2.4	40
45	Altered Composition of Bone as Triggered by Irradiation Facilitates the Rapid Erosion of the Matrix by Both Cellular and Physicochemical Processes. PLoS ONE, 2013, 8, e64952.	2.5	39
46	Bone Matrix Quality After Sclerostin Antibody Treatment. Journal of Bone and Mineral Research, 2014, 29, 1597-1607.	2.8	38
47	XANES Spectroscopy: A Promising Tool for Toxicology:. NeuroToxicology, 2002, 23, 127-146.	3.0	37
48	Determining the oxidation states of manganese in NT2 cells and cultured astrocytes. Neurobiology of Aging, 2006, 27, 1816-1826.	3.1	36
49	Dynamic Full-Field Infrared Imaging with Multiple Synchrotron Beams. Analytical Chemistry, 2013, 85, 3599-3605.	6.5	36
50	Characterization of Protein Structural Changes in Living Cells Using Time-Lapsed FTIR Imaging. Analytical Chemistry, 2015, 87, 6025-6031.	6.5	35
51	A new sample substrate for imaging and correlating organic and trace metal composition in biological cells and tissues. Analytical and Bioanalytical Chemistry, 2007, 387, 1705-1715.	3.7	33
52	Determining the oxidation states of manganese in PC12 and nerve growth factor-induced PC12 cells. Free Radical Biology and Medicine, 2005, 39, 164-181.	2.9	32
53	Following matrix metalloproteinases activity near the cell boundary by infrared micro-spectroscopy. Matrix Biology, 2002, 21, 567-577.	3.6	29
54	Overexpression of DMP1 accelerates mineralization and alters cortical bone biomechanical properties in vivo. Journal of the Mechanical Behavior of Biomedical Materials, 2012, 5, 1-8.	3.1	28

#	Article	IF	CITATIONS
55	X-ray Fluorescence Nanotomography of Single Bacteria with a Sub-15 nm Beam. Scientific Reports, 2018, 8, 13415.	3.3	28
56	Lanthanide-Binding Tags for 3D X-ray Imaging of Proteins in Cells at Nanoscale Resolution. Journal of the American Chemical Society, 2020, 142, 2145-2149.	13.7	27
57	Synchrotron Infrared Microspectroscopy Detecting the Evolution of Huntington's Disease Neuropathology and Suggesting Unique Correlates of Dysfunction in White versus Gray Brain Matter. Analytical Chemistry, 2011, 83, 7712-7720.	6.5	23
58	Alterations in Collagen and Mineral Nanostructure Observed in Osteoporosis and Pharmaceutical Treatments Using Simultaneous Small- and Wide-Angle X-ray Scattering. Calcified Tissue International, 2014, 95, 446-456.	3.1	21
59	Changes in protein structure and distribution observed at pre-clinical stages of scrapie pathogenesis. Biochimica Et Biophysica Acta - Molecular Basis of Disease, 2008, 1782, 559-565.	3.8	20
60	Interpretation of solution scattering data from lipid nanodiscs. Journal of Applied Crystallography, 2018, 51, 157-166.	4.5	19
61	Misfolded opsin mutants display elevated <i>β</i> â€sheet structure. FEBS Letters, 2015, 589, 3119-3125.	2.8	18
62	Timeâ€resolved xâ€ray absorption spectroscopy on microsecond timescales: Implications for the examination of structural motions. Review of Scientific Instruments, 1993, 64, 2035-2036.	1.3	16
63	Copper accumulation and the effect of chelation treatment on cerebral amyloid angiopathy compared to parenchymal amyloid plaques. Metallomics, 2020, 12, 539-546.	2.4	16
64	Biophysical and Structural Characterization of a Sequence-diverse Set of Solute-binding Proteins for Aromatic Compounds. Journal of Biological Chemistry, 2012, 287, 23748-23756.	3.4	15
65	Design and implementation of a rapid-mixer flow cell for time-resolved infrared microspectroscopy. Review of Scientific Instruments, 2000, 71, 4057.	1.3	14
66	Imaging Nutrient Distribution in the Rhizosphere Using FTIR Imaging. Analytical Chemistry, 2017, 89, 4831-4837.	6.5	12
67	Applications of infrared microspectroscopy to geology, biology and cosmetics. Synchrotron Radiation News, 1998, 11, 31-37.	0.8	10
68	The use of synchrotron infrared microspectroscopy in the assessment of cutaneous T-cell lymphoma vs. pityriasis lichenoides chronica. Photodermatology Photoimmunology and Photomedicine, 2010, 26, 93-97.	1.5	10
69	Bone Matrix Composition Following PTH Treatment is Not Dependent on Sclerostin Status. Calcified Tissue International, 2016, 98, 149-157.	3.1	8
70	<title>Analysis of bone protein and mineral composition in bone disease using synchrotron infrared microspectroscopy</title> . , 1999, , .		7
71	Fourier Transform Infrared Imaging as a Tool to Chemically and Spatially Characterize Matrix-Mineral Deposition in Osteoblasts. Calcified Tissue International, 2013, 92, 50-58.	3.1	7
72	Copper stabilizes antiparallel β-sheet fibrils of the amyloid β40 (Aβ40)-Iowa variant. Journal of Biological Chemistry, 2020, 295, 8914-8927.	3.4	7

0

#	Article	IF	CITATIONS
73	Development and applications of an epifluorescence module for synchrotron x-ray fluorescence microprobe imaging. Review of Scientific Instruments, 2005, 76, 066107.	1.3	6
74	Synchrotron infrared microspectroscopy as a means of studying the chemical composition of bone: applications to osteoarthritis. , 1997, , .		5
75	HBM Mice Have Altered Bone Matrix Composition and Improved Material Toughness. Calcified Tissue International, 2016, 99, 384-395.	3.1	5
76	Technical Report: The Diversity of Infrared Programs at the NSLS. Synchrotron Radiation News, 2007, 20, 25-34.	0.8	2
77	Infrared spectroscopy and imaging for understanding neurodegenerative protein-misfolding diseases. , 2020, , 121-142.		2
78	Discrimination Between Paraffin-Embedded and Frozen Skin Sections Using Synchrotron Infrared Microspectroscopy. International Journal of Peptide Research and Therapeutics, 2014, 20, 13-17.	1.9	1
79	<i>In situ</i> examination of osteoblast biomineralization on sulfonated polystyrene-modified substrates using Fourier transform infrared microspectroscopy. Biointerphases, 2017, 12, 031001.	1.6	1
80	Amide 1 Expression in Psoriasis and Lichen Planus using Synchrotron Infrared Microspectroscopy. International Journal of Peptide Research and Therapeutics, 2013, 19, 203-207.	1.9	0
81	Biochemical Changes Observed After PUVA Versus PUVA Plus Methotrexate Therapy in Mycosis Fungoides Using Synchrotron Infrared Microspectroscopy. International Journal of Peptide Research and Therapeutics, 2013, 19, 209-215.	1.9	0

82 Infrared Spectroscopy Using Synchrotron Radiation. , 2018, , 1-9.